



저작자표시-비영리-변경금지 2.0 대한민국

이용자는 아래의 조건을 따르는 경우에 한하여 자유롭게

- 이 저작물을 복제, 배포, 전송, 전시, 공연 및 방송할 수 있습니다.

다음과 같은 조건을 따라야 합니다:



저작자표시. 귀하는 원저작자를 표시하여야 합니다.



비영리. 귀하는 이 저작물을 영리 목적으로 이용할 수 없습니다.



변경금지. 귀하는 이 저작물을 개작, 변형 또는 가공할 수 없습니다.

- 귀하는, 이 저작물의 재이용이나 배포의 경우, 이 저작물에 적용된 이용허락조건을 명확하게 나타내어야 합니다.
- 저작권자로부터 별도의 허가를 받으면 이러한 조건들은 적용되지 않습니다.

저작권법에 따른 이용자의 권리는 위의 내용에 의하여 영향을 받지 않습니다.

이것은 [이용허락규약\(Legal Code\)](#)을 이해하기 쉽게 요약한 것입니다.

[Disclaimer](#)

A THESIS FOR THE DEGREE OF MASTER OF SCIENCE

**A study on the effect of freezing rate on
catalytic activity and molecular structure
of L-lactate dehydrogenase**

L-Lactate dehydrogenase 의 효소 활성 및 분자 구조
에 동결 속도가 미치는 영향에 관한 연구

August, 2019

**Department of Agricultural Biotechnology
Seoul National University
Haena Park**

석사학위논문

**A study on the effect of freezing rate on
catalytic activity and molecular structure
of L-lactate dehydrogenase**

지도교수 장 판 식

이 논문을 석사학위 논문으로 제출함

2019년 8월

서울대학교 대학원

농 생 명 공 학 부

박 해 나

박해나의 석사 학위논문을 인준함

2019년 8월

위원장 강 동 현 (인)

부위원장 장 판 식 (인)

위원 최 영 진 (인)

Abstract

The purpose of this study was to investigate the effect of freezing rate upon the catalytic activity of L-lactate dehydrogenase (LDH) and to propose optimal freezing rates for LDH. Structural changes to LDH at different freezing rates were analyzed to understand the enzyme deactivation process during the freezing process. A liquid-mediated freezing (LMF) system was established to control the freezing rate in this study. LMF is a novel freezing technique based on the simultaneous freezing of samples with the pre-cooled isopropyl alcohol (IPA). The freezing rate could be determined by the initial temperature of IPA before freezing.

Initially, the residual activity of LDH was about 80% at freezing rates of 0.2 – 3.8°C/min, and at higher freezing rates residual activity significantly decreased as the freezing rates increased ($p < 0.05$). The residual activities at freezing rates of 12.8 and 70.6°C/min were 64.1% and 44.8%, respectively. Changes in the quaternary structure of LDH were analyzed using blue native-PAGE. At 70.6°C/min, the intensities of the tetramer and dimer forms of LDH were weakened, so LDH was dissociated at the higher freezing rate. Changes in the tertiary structure of LDH were analyzed using fluorescence

spectroscopy. As the freezing rate increased, the fluorescence at 339 nm significantly decreased ($p < 0.05$) implying the presence of changes in the tertiary structure of LDH.

These results showed that the freezing could cause protein aggregation. The size distribution measured by dynamic light scattering analysis and fluorescence microscopy images of aggregates showed that larger aggregates were produced as the freezing rate increased. Finally, the increase of intrinsic protein fluorescence emitted at 563 nm suggested that protein aggregation by freezing would be amyloid.

This study showed that freezing rate is an important factor in maintaining catalytic activity during the freezing process, and suggested the optimum freezing rates for LDH. These results could be used to elucidate the mechanism of enzyme deactivation during the freezing process in further studies.

Keywords: Freezing process, L-Lactate dehydrogenase, freezing rate, structural change, protein aggregation

Student number: 2017-28564

Contents

Abstract.....	I
Contents.....	III
List of tables.....	V
List of figures.....	VI
1. Introduction	1
2. Materials and methods.....	4
2.1. Materials.....	4
2.2. Preparation of L-lactate dehydrogenase.....	4
2.3. L-Lactate dehydrogenase assay.....	5
2.4. Freezing and thawing process.....	6
2.4.1. Freezing process	6
2.4.2. Thawing process	6
2.4.3. Ice seeding.....	8
2.4.4. Temperature profiling.....	10
2.5. Blue native-PAGE and silver staining.....	10
2.6. Intrinsic fluorescence spectroscopy.....	11

2.7. Fluorescence microscopy	12
2.8. Dynamic light scattering (DLS).....	12
3. Results and discussions.....	13
3.1. The liquid-mediated freezing system controlling freezing rate.....	13
3.1.1. Principles of the liquid-mediated freezing system.....	13
3.1.2. Elimination of supercooling by ice seeding	18
3.2. Effect of the freezing rate on LDH activity.....	22
3.3. Structural changes in LDH by different freezing rates.....	25
3.3.1. Changes in the quaternary structure of LDH.....	26
3.3.2. Changes in the tertiary structure of LDH.....	29
3.4. Aggregate formation at different freezing rates.....	33
3.4.1. Size distribution of the aggregates.....	33
3.4.2. Visualization of the aggregates.....	36
3.4.3. Amyloid structure of the aggregates	38
4. Conclusions.....	41
5. References.....	42
국문초록.....	47

List of tables

Table 1. Supercooling points of the liquid-mediated freezing system at each initial temperature of isopropyl alcohol

Table 2. Freezing rates at each initial temperature of isopropyl alcohol

Table 3. Fluorescence emission wavelength (λ_{\max} , nm) of the L-lactate dehydrogenase after five freeze-thawing cycles

List of figures

Fig. 1. Schematic diagram of the experimental freeze-thawing process.

LMF, liquid-mediated freezing.

Fig. 2. Schematic diagram of the ice seeding. The nucleation temperature was -1°C .

Fig. 3. Schematic diagram of the liquid-mediated freezing system (a). T_I indicates the temperature of isopropyl alcohol (IPA), and T_S represents the temperature of the enzyme solution. The cooling curve of IPA (400 mL) placed in the deep freezer (-75°C) shelf (b).

Fig. 4. Freezing curves of L-lactate dehydrogenase (LDH) solution at different freezing conditions ($T_I = x^{\circ}\text{C}$, $x = -10, -20, -30, -40, \text{ and } -50$). T_I indicates the initial temperature of isopropyl alcohol. The concentration of LDH solution was $20 \mu\text{g/mL}$. LMF, liquid-mediated freezing.

Fig. 5. Freezing curves of L-lactate dehydrogenase solution with ice seeding at the different freezing methods. LMF, liquid-mediated freezing.

Fig. 6. Effect of the freezing rates on the catalytic activities of L-lactate dehydrogenase. Asterisks (*) indicate significant differences ($p < 0.05$). NS indicates non-significant differences.

Fig. 7. Blue native-PAGE and silver staining of L-lactate dehydrogenase (LDH) before and after freeze-thawing cycles for 6 times. The concentration of the LDH solution was 40 $\mu\text{g}/\text{mL}$. Lane 1 was for untreated LDH. Lane 2, 3, and 4 were for freeze-thawed LDH at the freezing rates of 0.2, 12.8, and 70.6 $^{\circ}\text{C}/\text{min}$.

Fig. 8. Intrinsic fluorescence emission spectra of 20 $\mu\text{g}/\text{mL}$ L-lactate dehydrogenase (LDH) before and after five freeze-thawing cycles. The LDH solutions were frozen at a rate of 0.2, 12.8, and 70.6 $^{\circ}\text{C}/\text{min}$. The excitation wavelength was 280 nm.

Fig. 9. The size distributions of freeze-thawed LDH. The refractive index chosen for the particles was the protein presetting, and the refractive index of the medium was approximated to be that of water.

Fig. 10. Nile red fluorescence micrographs of 20 $\mu\text{g}/\text{mL}$ L-lactate dehydrogenase before and after freeze-thawing cycles for five times. The untreated LDH is represented in (a). The freezing rates were 0.2 $^{\circ}\text{C}/\text{min}$ (white arrows indicate red particles) (b), 12.8 $^{\circ}\text{C}/\text{min}$ (c), and 70.6 $^{\circ}\text{C}/\text{min}$ (d).

Fig. 11. Intrinsic fluorescence emission spectra of 20 $\mu\text{g}/\text{mL}$ L-lactate dehydrogenase before and after five freeze-thawing cycles at the visible range. The LDH solutions were frozen at 0.2, 12.8, and 70.6 $^{\circ}\text{C}/\text{min}$. The excitation wavelength was 280 nm.

1. Introduction

Lyophilization is a commonly-used method for the storage of enzymes which are unstable in solution (Kasper & Friess, 2011). In the sublimation step of lyophilization, more than 95% of water can be removed, and consequently physicochemical degradation is suppressed, resulting in the improvement of storage stability (Kasper & Friess, 2011). However, several enzymes lose their catalytic activities after lyophilization because of physicochemical damages occurring during the freezing and drying processes (Bhatnagar, Pikal, & Bogner, 2008).

Previous studies into lyophilization have focused on the drying process rather than on the freezing process (Kasper & Friess, 2011), since the drying process takes much more energy and time than the freezing process. However, the freezing process is also important, due to its effects on the catalytic activity of enzymes. Physicochemical changes such as ice formation, and freeze-concentration that occur during the freezing process can cause irreversible changes in the structures of proteins (Bhatnagar, Bogner, & Pikal, 2007). During the freezing process, an interface between ice and an unfrozen solution is formed. These interfacial areas need to be adjusted by manipulation of the

freezing rate, because proteins tend to lose their structural stability when they are located in the interface (Chang, Kendrick, & Carpenter, 1996). At high freezing rates, numerous small ice crystals form a large interfacial area in which proteins are more susceptible to damage (Bhatnagar, Pikal, & Bogner, 2008). Therefore, the freezing rate should be considered as a significant factor during the freezing process for enzymes.

There is a lack of systematic studies about the effect of the freezing rate on the catalytic activity of enzymes during freezing (Cao, Chen, Cui, & Foster, 2003), and the mechanism of deactivation by freezing has not been clearly elucidated. Most of the freezing studies have focused on empirical analysis using various cryoprotectants (Bhatnagar, Pikal, & Bogner, 2008; Franks, 1992), although the use of the cryoprotectants are still limited in that they affect the quality and purity of the products (Cao, Chen, Cui, & Foster, 2003). Therefore, more research is needed to investigate the relationship between enzyme deactivation and freezing.

The purpose of this study was to investigate the effect of freezing rate on the catalytic activity of L-lactate dehydrogenase (LDH), and to identify the optimal freezing rates for LDH in terms of enzyme activity. In this study, a liquid-mediated freezing (LMF) system was established in order to control the freezing rate. Through the LMF system, freezing rates were controlled in a

convenient and reproducible manner. L-Lactate dehydrogenase (LDH, EC 1.1.1.27) was used as a model enzyme because it is known to lose its catalytic activity after freezing or lyophilization (Kasper & Friess, 2011). The structural changes to LDH induced by freezing were analyzed using blue native-PAGE, fluorescence spectroscopy, dynamic light scattering, and fluorescence microscopy in order to elucidate the mechanism of the deactivation.

2. Materials and methods

2.1. Materials

L-Lactate dehydrogenase (LDH) Type II, from rabbit muscle as an aqueous ammonium sulfate suspension, β -Nicotinamide adenine dinucleotide (NADH) in a reduced form of greater than 97% purity, tris base, methylene-bis-acrylamide, tricine, bis-tris, and formaldehyde were purchased from Sigma Chemical Co. (St. Louis, MO, USA). Pyruvate of greater than 98% purity was obtained from Kanto Chemical Co. (Tokyo, Japan.). Acrylamide and Coomassie Brilliant Blue G-250 used was of BioRad electrophoresis grade. All other chemicals were of analytical grade.

2.2. Preparation of L-lactate dehydrogenase

The commercial LDH product, a crystalline suspension in 3.2 M ammonium sulfate (NH_4) SO_2 solution, was used without removing the (NH_4) SO_2 , and LDH was dissolved in 0.2 M Tris-HCl buffer (pH 7.4) for assay. The concentration of the protein was determined by measuring the absorbance at 280 nm and 260 nm as described below.

$$\text{Protein concentration (mg/mL)} = 1.55 \times A_{280} - 0.76 \times A_{260}$$

Samples used for quantifying the protein concentration were run in duplicate

and 1 mL was used for each measurement.

2.3. L-Lactate dehydrogenase assay

Catalytic activity was measured by the Worthington Biochemical Corporation (Lakewood, NJ), based on the conversion of pyruvate to lactate by LDH. The reaction was performed in 0.2 M Tris-HCl buffer at 25°C (pH 7.4), and the product was measured using a spectrophotometer (UV-2450, Shimadzu, Japan). The reaction mixture consisted of 11.4 mL of 0.2 M Tris-HCl buffer (pH 7.4), 0.4 mL of 6.6 mM NADH, and 0.4 mL of 30 mM pyruvate. The reaction was initiated by the addition of 0.4 mL of 1.8 µg/mL LDH. The NADH and pyruvate used as the substrate were dissolved in the buffer within two hours before use. Catalytic activity was calculated by the rate of decrease in absorbance of NADH at 340 nm. The samples were run in triplicate, and the residual activity was calculated as described below.

$$\text{Residual activity (\%)} = \frac{v_a}{v_b} \times 100$$

(v_a =Initial velocity after freeze-thawing,

v_b =Initial velocity before freeze-thawing)

2.4. Freezing and thawing process

2.4.1. Freezing process

All of the enzyme samples were frozen in 2 mL polypropylene Eppendorf tubes, and 1 mL of sample was loaded per tube. All of the samples were treated with ice seeding before freezing. In this study, three different freezing methodologies were used: (1) conventional freezing achieved by placing samples directly on the deep freezer (-75°C) shelf; (2) liquid-mediated freezing (LMF) by immersing samples in pre-cooled IPA (See Fig. 3), and (3) freezing in liquid nitrogen by immersing samples in liquid nitrogen for 10 minutes followed by transfer to a deep freezer (-75°C) shelf. In the LMF system, the freezing rates were controlled by adjusting the initial temperature of the IPA. The total freezing time was two hours in all cases.

2.4.2. Thawing process

Thawing was conducted in the 25°C water bath for four minutes, at a thawing rate of 14°C/min. The overall freeze-thawing procedure is described in Fig. 1. The freeze-thawing process was done for one to several times.

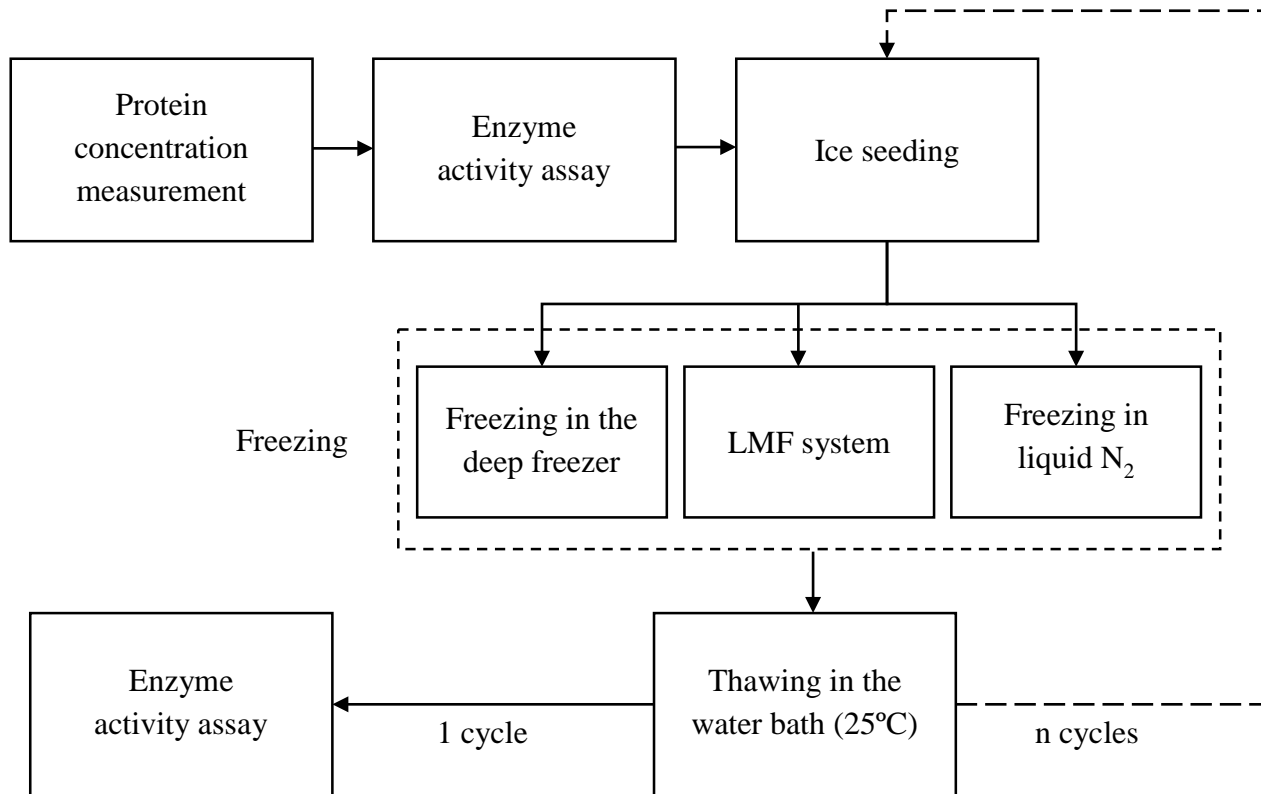


Fig. 1. Schematic diagram of the experimental freeze-thawing process. LMF, liquid-mediated freezing.

2.4.3. Ice seeding

Enzyme samples were pre-cooled to -1°C for two minutes in a chilling block (Cole-Parmer Benchtop, Vernon Hills, IL, USA). This temperature is below that of the freezing point of the solution. A sterilized awl was held over the liquid nitrogen for 35 seconds, and at the end of the two minutes holding time, the pre-cooled awl was rapidly dipped into the sample (Fig. 2). After ice seeding, all samples were immediately frozen.

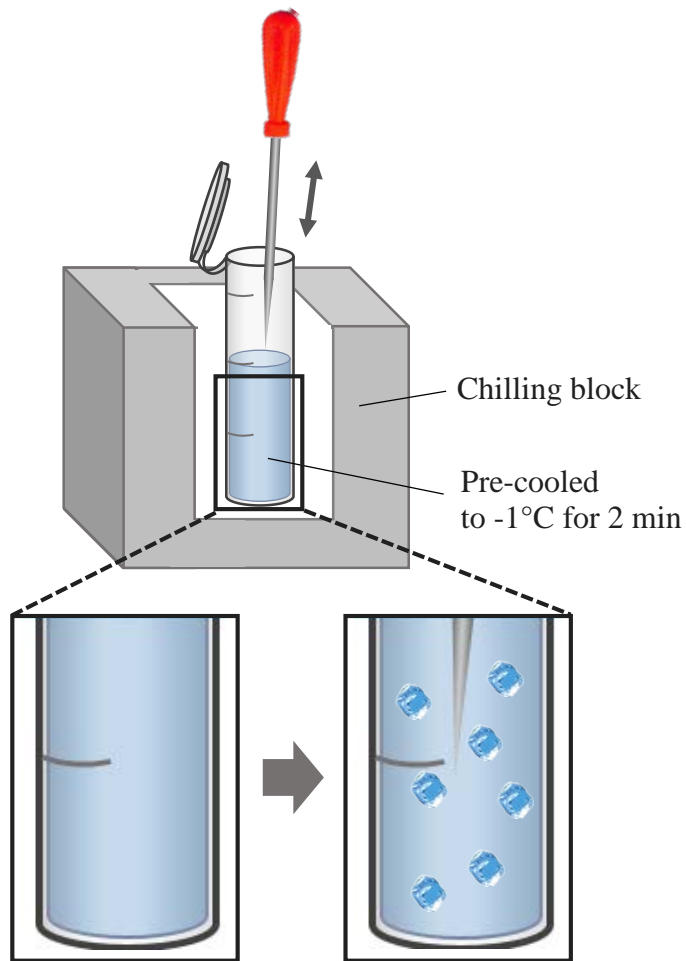


Fig. 2. Schematic diagram of the ice seeding.
The nucleation temperature was -1°C .

2.4.4. Temperature profiling

The temperature profile was measured using a data logger for type K thermocouples (MTM-380SD, Lutron, Taiwan). The temperature was measured every five seconds. The temperature profiles of IPA (400 mL) and enzyme samples were measured by placing the thermocouples inside the middle of the container, covered by a polystyrene lid. The freezing rate was defined as the rate at which crystals grew after ice nucleation (Kasper & Friess, 2011). Therefore, in this study, the freezing rates were expressed as a temperature change per unit hour in the zone of maximum ice crystal formation, where most ice crystals are produced.

$$\text{Freezing rate (}^{\circ}\text{C/min)} = \frac{T_2 - T_1}{t_2 - t_1}$$

($T_1 = 0^{\circ}\text{C}$, $T_2 = -5^{\circ}\text{C}$, and is the time elapsed between t_1 and t_2)

2.5. Blue native-PAGE and silver staining

Blue native-PAGE (BN-PAGE) was carried out using 0.002% (w/v) Coomassie blue G-250 for the cathode buffer (pH 7.0) with 3.3% polyacrylamide for the stacking gel (pH 7.0) and 6.5% polyacrylamide for the resolving gel (pH 7.0). The concentration of the enzyme solution for BN-

PAGE was 40 $\mu\text{g}/\text{mL}$. Electrophoresis was conducted at 90V for four hours at 4°C. After electrophoresis, the gel was incubated in the fixer solution (40% (v/v) ethanol, 10% (v/v) acetic acid) for one hour, and then washed in distilled water for nine hours. The gel was sensitized in 0.02% (w/v) sodium thiosulfate for one minute. Silver staining was conducted in 0.1% (w/v) silver nitrate solution in a 4°C refrigerator with a gentle rocking motion. The gel was developed in a solution consisting of 3% (w/v) sodium carbonate and 0.05% (v/v) formaldehyde. The formaldehyde was added just before use. Development was terminated by the addition of 5% (v/v) acetic acid solution.

2.6. Intrinsic fluorescence spectroscopy

Fluorescence spectra were measured using a fluorescence spectrometer (FluoroMate FS-2, Scinco Co., Seoul, Korea). The excitation was set to 280 nm, and the emission wavelength was scanned from 305 nm to 600 nm with 0.4 nm intervals using 5 nm/5 nm slit widths. The photomultiplier tube (PMT) voltage was set to 400 V, and the PMT integration time was 20 milliseconds. The concentration of the enzyme solution for fluorescence analysis was 20 $\mu\text{g}/\text{mL}$, and 1 mL of samples was used for each measurement.

2.7. Fluorescence microscopy

Fluorescence micrographs were obtained using a fluorescence microscope (DE/Axio Imager A1, Carl Zeiss, Oberkochen, Germany). Before measurement, 1 μL of 100 μM Nile Red dissolved in ethanol was added to 100 μL of enzyme sample. The concentration of the enzyme sample for fluorescence microscopy was 20 $\mu\text{g}/\text{mL}$. After the addition of Nile Red, the samples were placed on microscope slides (Deckglaser, Germany) and observed by microscopy. A Zeiss filter set 15 was used, and the images were acquired with an Axio Cam HRC CCD camera (Carl Zeiss). Micrographs were processed using the AxioVision Rel 4.8 software (Carl Zeiss). The observations were performed using the 100x oil immersion objective (EC Plan-Neofluar 100x/1.3 oil, Carl Zeiss).

2.8. Dynamic light scattering (DLS)

The size distribution of enzyme samples was analyzed by dynamic light scattering (DLS) using a Zetasizer Nano ZS90 (Malvern Instruments Ltd, Worcestershire, UK). The enzyme concentration of the frozen samples was 120 $\mu\text{g}/\text{mL}$, and 1 mL of each sample was used for measurement. All measurements were carried out at 4°C at a fixed angle of 90°.

3. Results and Discussions

3.1. The liquid-mediated freezing system controlling freezing rate

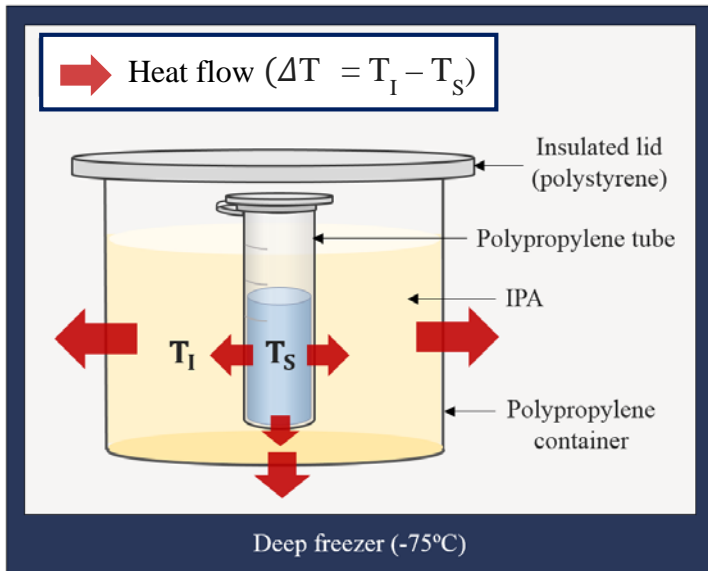
3.1.1. Principles of the liquid-mediated freezing system

In this study an LMF system that can control the freezing rate was developed (Fig. 3 (a)). LMF is a freezing technology based on the simultaneous cooling of an enzyme and an organic solvent (IPA). The temperature of the IPA at the beginning of freezing is lower than the temperature of the sample, and consequently heat flows from the sample into the solvent (small red arrows in Fig. 3 (a)) during freezing. According to Fourier's first law of heat transfer, the freezing rate of the sample depends upon the temperature difference between the solvent (T_I) and the sample (T_S). As ΔT ($\Delta T = T_I - T_S$) increases, the heat transfer rate becomes higher, leading to higher freezing rates. Therefore, the freezing rate can be controlled by ΔT , and can be adjusted by T_I . Since the specific heat is always constant, holding the initial temperature of the solvent and the deep freezer before cooling, the solvent always cools according to a uniform pattern. With this consistent cooling curve of the IPA, the initial temperature of the solvent was adjusted. IPA was suitable for this study because it has a low freezing point (-89°C) and a high specific heat ($0.596 \text{ Kcal/Kg}\cdot^\circ\text{C}$). The IPA temperature

profile starting from 25°C in the deep freezer (-75°C) is shown in Fig. 3 (b).

The temperature profiles of the LDH solution at each initial temperature of IPA (T_I) are shown in Fig. 4. The lower the T_I value, the faster the freezing rates; however, supercooling occurred. As shown in Table 1, the degree of supercooling was noticeable at slow freezing rates. In general, the degree of supercooling increased as the freezing rate decreased and the rate of production of nuclear crystals increased as the degree of supercooling increased, resulting in a large number of nuclei (Bhatnagar, Bogner, & Pikal, 2007; Kasper & Friess, 2011). Because there is a limit to the growth of ice crystals, nuclei can form small ice crystals. Conversely, as the degree of supercooling decreases, the size of ice crystals increases (Bhatnagar, Bogner, & Pikal, 2007; Searles, Carpenter, & Randolph, 2001). The freezing rate and ice crystal size are generally in an inverse relationship; however, if supercooling occurs, this inverse relationship would be offset. Therefore, it was necessary to control the supercooling so that the ice crystal size could be determined only by the freezing rate.

(a)



(b)

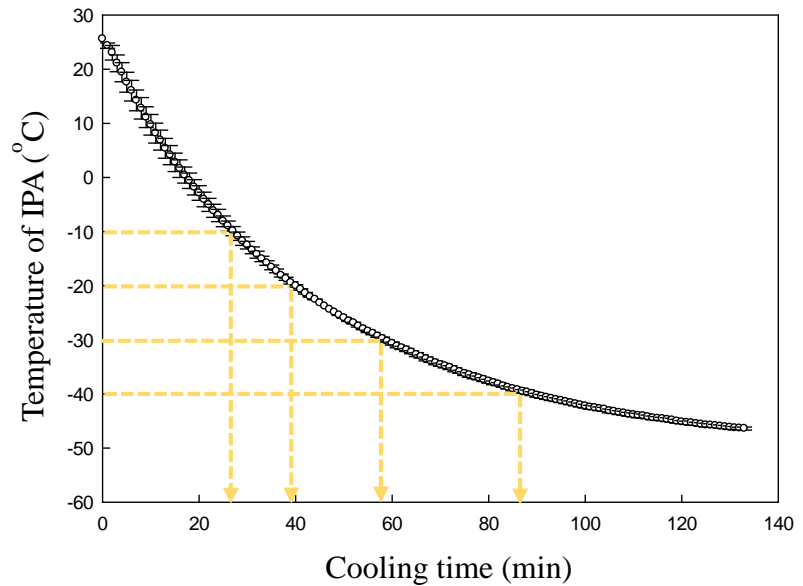


Fig. 3. Schematic diagram of the liquid-mediated freezing system (a). T_I indicates the temperature of isopropyl alcohol (IPA), and T_S represents the temperature of the enzyme solution. The cooling curve of IPA (400 mL) placed in the deep freezer (-75°C) shelf (b).

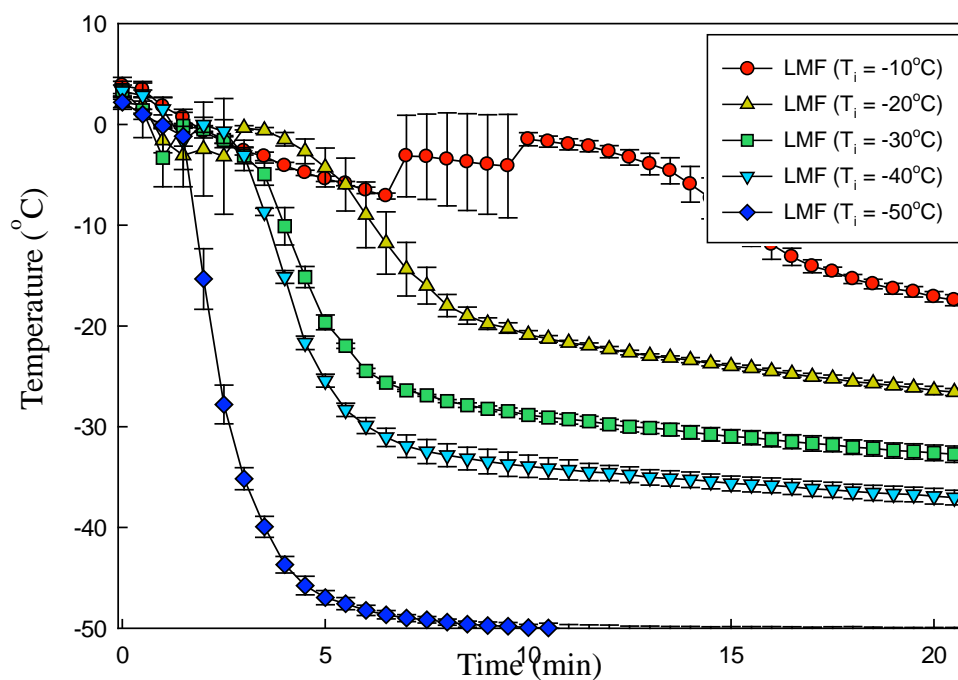


Fig. 4. Freezing curves of L-lactate dehydrogenase (LDH) solution at different freezing conditions ($T_i = x^\circ\text{C}$, $x = -10, -20, -30, -40,$ and -50). T_i indicates the initial temperature of isopropyl alcohol. The concentration of LDH solution was $20 \mu\text{g/mL}$. LMF, liquid-mediated freezing.

Table 1. Supercooling points of the liquid-mediated freezing system at each initial temperature of isopropyl alcohol

Initial temperature of IPA (°C)	Supercooling point (°C)
-10	-8.2 ± 1.3
-20	-6.6 ± 2.5
-30	-7.2 ± 1.3
-40	-2.8 ± 2.0
-50	ND*

*ND, Not detected.

IPA, isopropyl alcohol.

3.1.2. Elimination of supercooling by ice seeding

In this study, the ice seeding technique was applied as a pre-freeze to eliminate supercooling. Fig. 5 showed that supercooling did not occur by ice seeding. The freezing rates of each condition were calculated in this non-supercooling condition (Table 2).

In general, pure water does not freeze spontaneously at its equilibrium freezing point, and supercooling always occurs because nuclei, which must be formed in order to produce ice crystal growth, form well at lower temperatures (Kasper & Friess, 2011). Ice seeding, which can form ice nuclei, can be used to lower or eliminate this supercooling (Wilson, Heneghan, & Haymet, 2003). During the lowering of the temperature of the samples to slightly lower than the freezing point (-1°C in this experiment), the sample exists in a metastable state which does not produce spontaneous nucleation, but which allows ice crystals to grow (Wilson, Heneghan, & Haymet, 2003). In this metastable state, once the nuclei are formed by rapidly streaking an extremely pre-cooled awl, ice nucleation can start from the nuclei (Wilson, Heneghan, & Haymet, 2003) and supercooling does not occur as in the results. Ice seeding also improves the reproducibility of ice crystal formation. Ice crystal size is heterogeneous, because ice nucleation occurs stochastically (Kasper & Friess, 2011); however, if the ice seeding makes consistent nuclei, relatively uniform size can be

obtained under the same freezing conditions (Kasper & Friess, 2011).

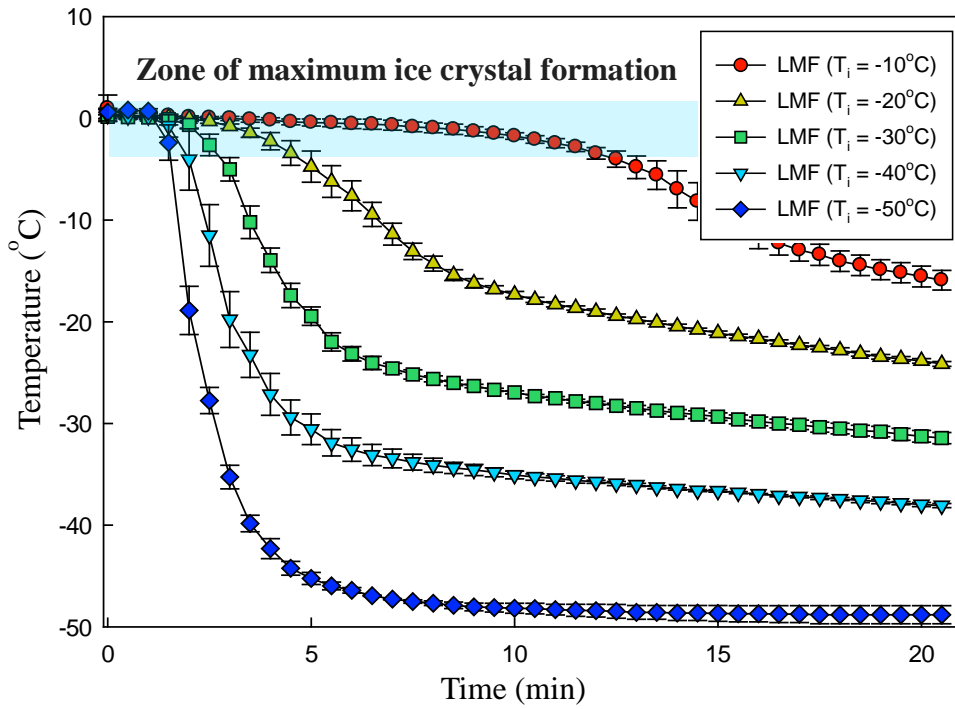


Fig. 5. Freezing curves of L-lactate dehydrogenase solution with ice seeding at the different freezing methods. LMF, liquid-mediated freezing.

Table 2. Freezing rates at each initial temperature of isopropyl alcohol

Initial temperature of IPA (°C)	Freezing rate (°C/min)
-10	0.43 ± 0.04
-20	1.23 ± 0.19
-30	2.45 ± 0.41
-40	3.76 ± 2.06
-50	12.79 ± 3.30

IPA, isopropyl alcohol.

3.2. Effect of the freezing rate on LDH activity

As shown in Fig. 1, the freezing rate produced by freezing in the deep freezer shelf was slower than the LMF system, and the freezing rate produced by freezing in liquid nitrogen was faster than LMF. The residual activities at each freezing rate are shown in Fig. 6. The degree of activity loss of LDH was minimized without any significant differences at slow freezing rates range from 0.4 to 3.8°C/min ($p < 0.05$); however, it was significantly increased at higher freezing rates ($p < 0.05$).

Although the mechanism of enzyme deactivation during the freezing process has not been clearly interpreted (Zhang, Qi, Singh, & Fernandez, 2011), the most popular hypothesis is that proteins present in the interfacial area between the ice crystal and the unfrozen portion lose their activity when adsorbed to the ice interface (Schwegman, Carpenter, & Nail, 2009). Most of the proteins have very complex structures with amphipathic properties containing combinations of ionic, polar, and non-polar regions, and they can bind to a variety of materials (Dickinson, 1999). They can therefore be readily adsorbed to an ice/unfrozen aqueous interface, leading to activity loss (Dickinson, 1999). Therefore, it seems that as the area of the ice/unfrozen aqueous interface becomes large, the number of enzymes placed at the interface will increase, and the enzymes could lose some of their activity. The

results of this study are in keeping with this hypothesis. It shows that the faster the freezing rate, the smaller the size of the ice crystals, leading to an increase in the interfacial area and consequent enzyme deactivation (Searles, Carpenter, & Randolph, 2001). Therefore, it seems to be essential to adjust the interfacial area by controlling the freezing rate in order to minimize the loss of enzyme activity.

Slow freezing rates are not optimum for lyophilization, because a long freezing process tends to produce large ice crystals and lower the evaporation efficiency of the drying process. Optimal freezing rates can also be different for each protein. For freeze-labile enzymes which would be expected to have a structure adsorbed well on the interface with high flexibility, the optimal freezing rates could be in a low temperature range. For enzymes with a high resistance to the interface, the optimal freezing rates could be high. It appears to be essential to adjust the optimal freezing rates to the structural characteristics of each protein.

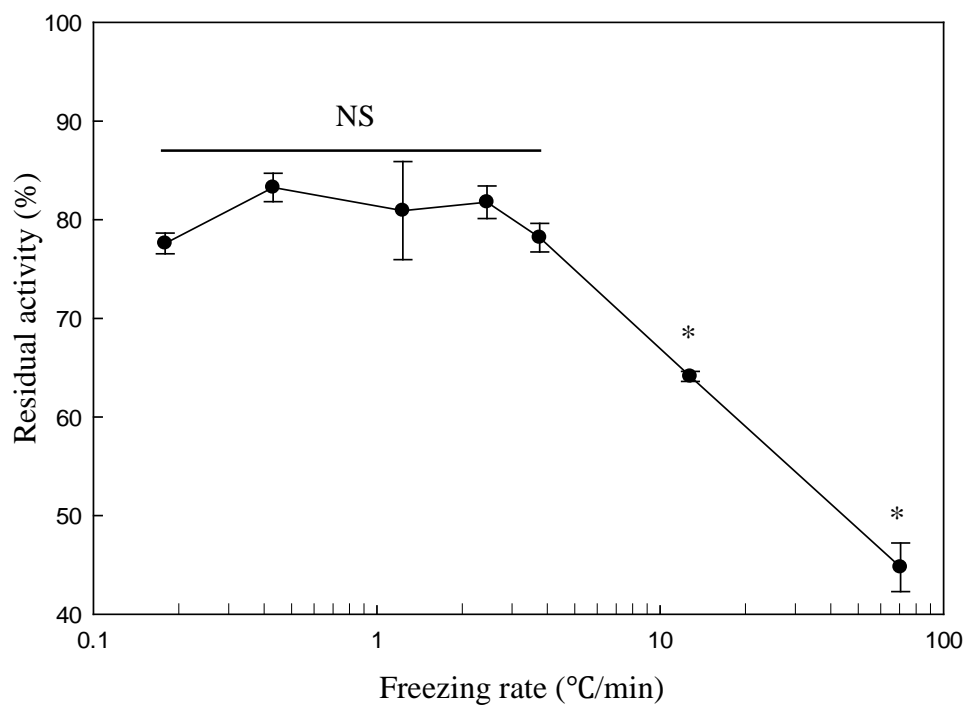


Fig. 6. Effect of the freezing rates on the catalytic activities of L-lactate dehydrogenase. Asterisks (*) indicate significant differences ($p < 0.05$). NS indicates non-significant differences.

3.3. Structural changes in LDH by different freezing rates

These results showed that the freezing rate is an important factor for the catalytic activity of LDH during the freezing process, and suggested that the cause of the loss of activity could be structural changes (Pikal-Cleland, Rodriguez-Hornedo, Amidon, & Carpenter, 2000). In this study, a comparative analysis of the protein structures before and after freeze-thawing was carried out to investigate how the freezing rate affects the enzyme structures. The experiments were conducted under freezing rates of 0.2, 12.8, and 70.6°C/min, all of which showed significant differences in residual activity.

Recent research suggests that multimeric enzymes tend to lose enzymatic activity after dissociation (Pikal-Cleland, Rodriguez-Hornedo, Amidon, & Carpenter, 2000). The model enzyme LDH, which is composed of four subunits, is deactivated when it loses its quaternary structure (Anchordoquy & Carpenter, 1996; Pikal-Cleland, Rodriguez-Hornedo, Amidon, & Carpenter, 2000). It has been shown that LDH is prone to dissociation by freezing-induced damage, resulting in its deactivation (Anchordoquy, Izutsu, Randolph, & Carpenter, 2001). For these reasons, analysis of quaternary structure using BN-PAGE was performed in order to investigate the effects of freezing rates on the extent of dissociation. Moreover, since the dissociated monomer form can easily be unfolded due to its low stability (Pikal-Cleland, Rodriguez-

Hornedo, Amidon, & Carpenter, 2000), the intrinsic protein fluorescence of LDH was analyzed to identify overall tertiary structural changes.

3.3.1. Changes in the quaternary structure of LDH

Blue native-PAGE (BN-PAGE), a kind of non-reducing electrophoresis, enables the resolution of protein complexes into their molecular weights while minimizing dissociation, and facilitates the analysis of the degree of dissociation at each freezing rate (Wittig, Braun, & Schägger, 2006). Using Coomassie dye, which can bind to proteins, proteins can be charged and migrate to the anode (Wittig, Braun, & Schägger, 2006). However, dissociation cannot be completely prevented in the case of multimeric proteins maintaining their structure by labile hydrophobic interactions due to the anionic charge of the Coomassie dye (Wittig, Braun, & Schägger, 2006). As shown in Fig. 7, bands of monomers, dimers, and tetramers appeared on the gel even with the untreated protein sample.

The bands representing tetramers and dimers were significantly weakened at 70.6°C/min, the fastest freezing rate, at which the extent of dissociation is increased. It was difficult to identify significant differences between the sample frozen at these freezing rates (0.4, 12.8°C/min) and an untreated sample. However, the intensity of the monomer band in the 70.6°C/min lane

was not much darker, as the tetramer and dimer bands were weakened. It seems that some of the proteins were aggregated so that they could not migrate through the gel during electrophoresis, and were just stuck in the well. Dissociated subunits could easily be unfolded because the structural stability of their dissociated subunits is lower than the stability of intact multimeric proteins, and these unfolded monomers easily form aggregates by non-covalent interactions (Anchordoquy, Izutsu, Randolph, & Carpenter, 2001; Bulawa, Connelly, Devit, Wang, Weigel, Fleming, et al., 2012).

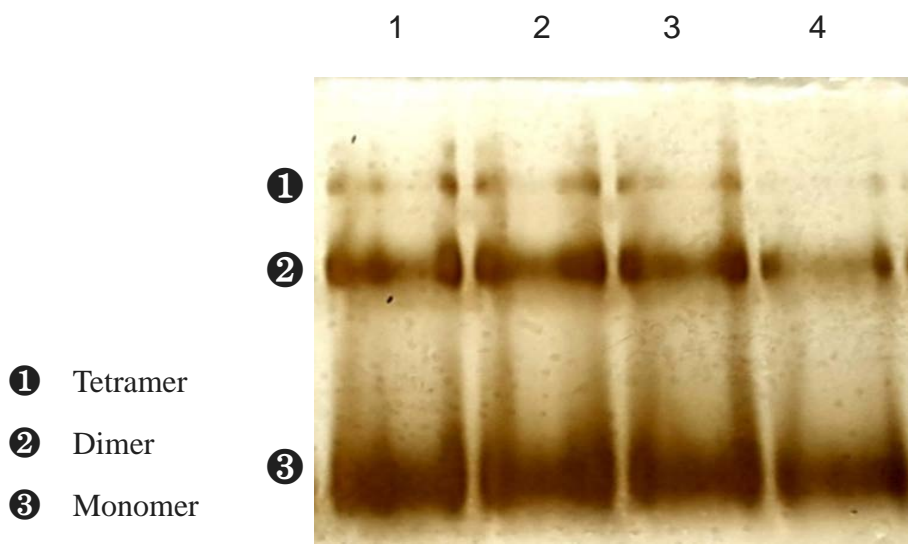


Fig. 7. Blue native-PAGE and silver staining of L-lactate dehydrogenase (LDH) before and after freeze-thawing cycles for 6 times. The concentration of the LDH solution was 40 $\mu\text{g}/\text{mL}$. Lane 1 was for untreated LDH. Lane 2, 3, and 4 were for freeze-thawed LDH at the freezing rates of 0.2, 12.8, and 70.6°C/min.

3.3.2. Changes in the tertiary structure of LDH

Fluorescence spectroscopy was used to analyze changes in the tertiary structures of LDH according to freezing rates. The fluorescence properties of tryptophan (Trp) and tyrosine (Tyr) in proteins can be used to measure structural changes in proteins (Royer, 2006) because their fluorescence properties are sensitive to their surroundings, and change when the protein is folded or unfolded. In a hydrophobic environment like that occurring in the core of a protein, Trp and Tyr have a high quantum yield and show a high fluorescence intensity (Royer, 2006); however, in a hydrophilic environment, such as when these proteins are unfolded, their quantum yield decreases, resulting in low intensity of fluorescence (Royer, 2006). Any changes in protein structure which affect the environment of the residues can be reflected as a change in the fluorescence intensity (Permyakov & Uversky, 2010). The maximum emission wavelength (λ_{\max}) can be used to measure protein conformational stability (Permyakov & Uversky, 2010) because when the environment of Trp is less polar, the Stokes shift will be less pronounced than in a more polar area (Permyakov & Uversky, 2010).

The intrinsic protein fluorescence emission spectra of LDH treated at different freezing rates are shown in Fig. 8. An increase in freezing rate

resulted in significant decreases in fluorescence intensity, indicating that the tertiary structure of LDH was changed as the freezing rate increased. Table 3 shows that λ_{\max} was different at 12.8 and 70.6°C/min, but it was a small change compared to the degree of shift, when the proteins are substantially unfolded. The results of BN-PAGE, seem to be due to protein aggregation. The LDH has many Trp residues on its surface (Duy & Fitter, 2006). Interactions of LDH usually transfer Trp residues to a more hydrophobic surrounding, which results in a blue shift in the maximum fluorescence position as found in this study (Duy & Fitter, 2006).

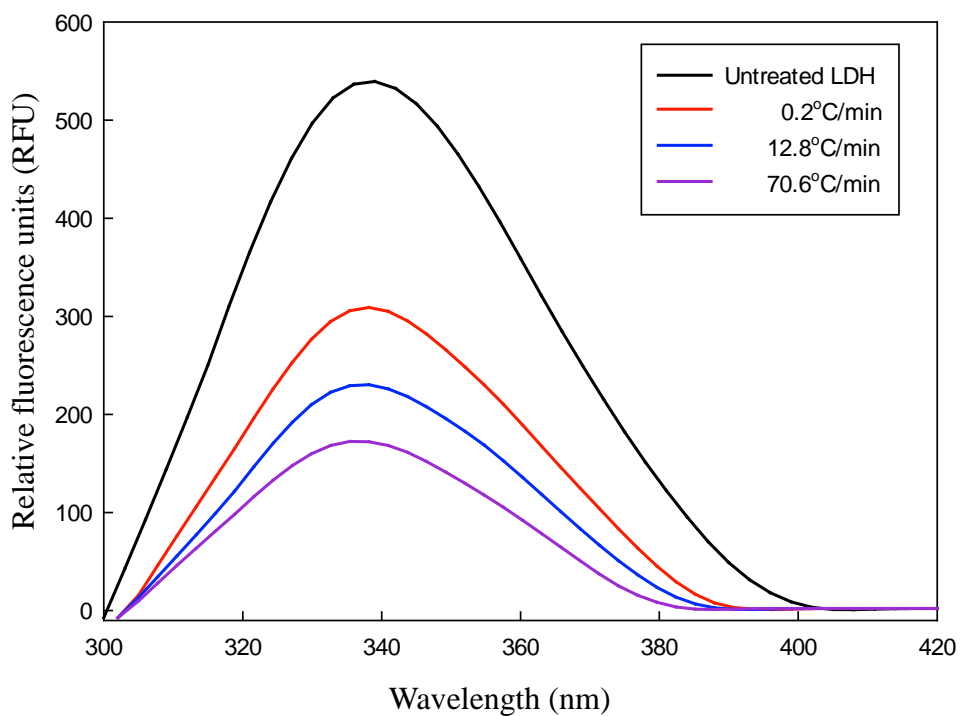


Fig. 8. Intrinsic fluorescence emission spectra of 20 $\mu\text{g/mL}$ L-lactate dehydrogenase (LDH) before and after five freeze-thawing cycles. The LDH solutions were frozen at a rate of 0.2, 12.8, and 70.6°C/min. The excitation wavelength was 280 nm.

Table 3. Fluorescence emission wavelength (λ_{max} , nm) of the L-lactate dehydrogenase after five freeze-thawing cycles

Freezing rate (°C/min)	λ_{max} (nm)	Changes in λ_{max} (nm)
0.2	338 ± 0.44	-1
12.8	337 ± 0.90	-2
70.6	336 ± 1.18	-3

3.4. Aggregates formation at different freezing rates

In this study, the degree of aggregation of LDH increased, in addition to structural changes at fast freezing rates. To analyze the aggregation of LDH according to freezing rates, DLS analysis, intrinsic fluorescence spectroscopy, and fluorescence microscopy were conducted.

3.4.1. Size distribution of the aggregates

In order to confirm whether protein aggregates were formed after freeze-thawing, the size distribution of the LDH solution was measured using DLS, which can measure colloid systems like protein solutions (den Engelsman, Garidel, Smulders, Koll, Smith, Bassarab, et al., 2011). According to Rayleigh's approximation, the intensity of a particle is proportional to the sixth power of its diameter, since large particles scatter much more light than small particles (Brar & Verma, 2011). Large particles can be easily detected through their scattering intensity, even if the particles exist in trace amounts. However, in a multimodal distribution, the intensity results tend to be distorted towards large particles because of their high sensitivity, so it is difficult to obtain an accurate size distribution (Lorber, Fischer, Bailly, Roy, & Kern, 2012). Therefore, the size distributions were expressed by volume converted from intensity to produce less emphasis on large particles. The measurement was

carried out at 4°C because DLS is affected by temperature, and low temperature could minimize protein aggregation.

The size distributions of the LDH solution at each freezing rate are shown in Fig. 9. Comparing the average diameter of untreated LDH (0.6 nm, data not shown), aggregation was induced in all treatment groups. At the slowest freezing rate (0.2°C/min), most particles had a diameter of around 10 nm. At faster freezing rates (12.8 and 70.6°C/min), the proportion of particles with a size around 1000 nm increased markedly. These results indicated that as the freezing rate increases, the proteins form more aggregates. It is reasonable to assume that proteins underwent structural changes by freezing and consequently formed aggregations.

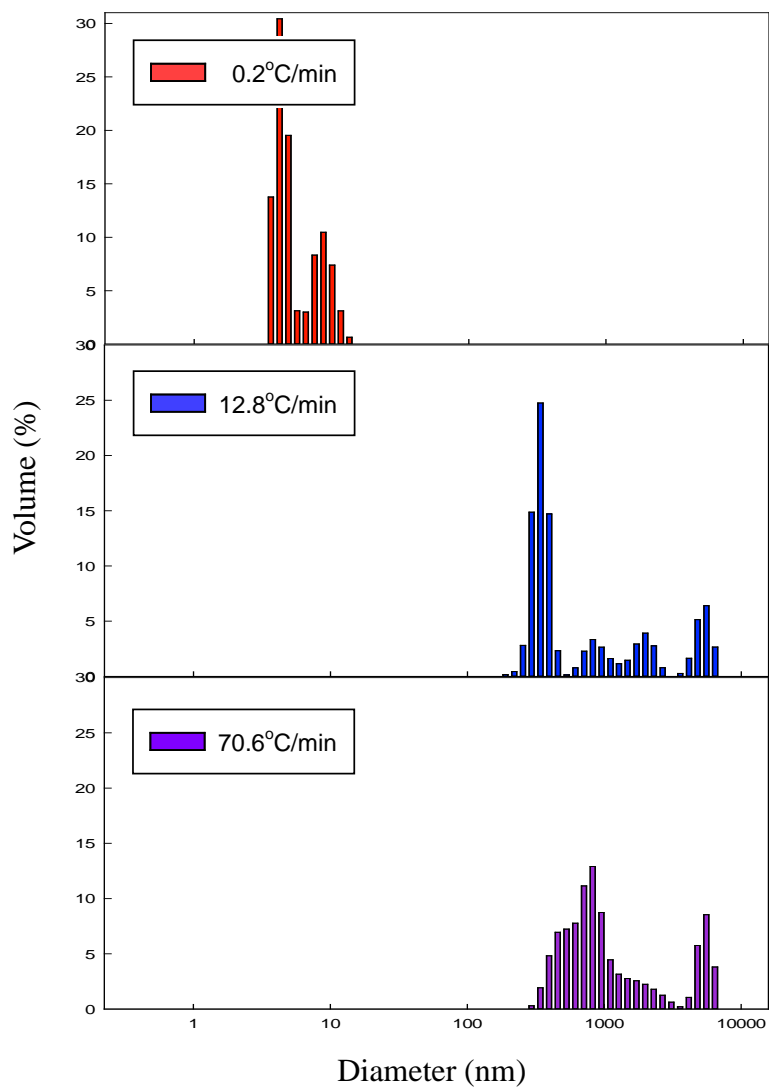


Fig. 9. The size distributions of freeze-thawed LDH. The refractive index chosen for the particles was the protein presetting, and the refractive index of the medium was approximated to be that of water.

3.4.2. Visualization of the aggregates

In this study, to visualize the aggregation of LDH at different freezing rates, the LDH samples were stained with Nile Red and then observed using a fluorescence microscope. Nile Red binds easily to hydrophobic surfaces which are exposed during protein unfolding or protein oligomerization and amyloid fibrillation (Demeule, Gurny, & Arvinte, 2007). When Nile Red is in such a hydrophobic environment, its quantum yield becomes higher, exhibiting strong fluorescence, whereas in hydrophilic solvent Nile Red is relatively undissolved, and its fluorescence is strongly quenched (Demeule, Gurny, & Arvinte, 2007). Therefore, through the Nile Red staining, it was possible to selectively detect aggregates. Consistent with observations from DLS results, the fluorescence intensity and the size of each particle increased as the freezing rate increased (Fig. 10).

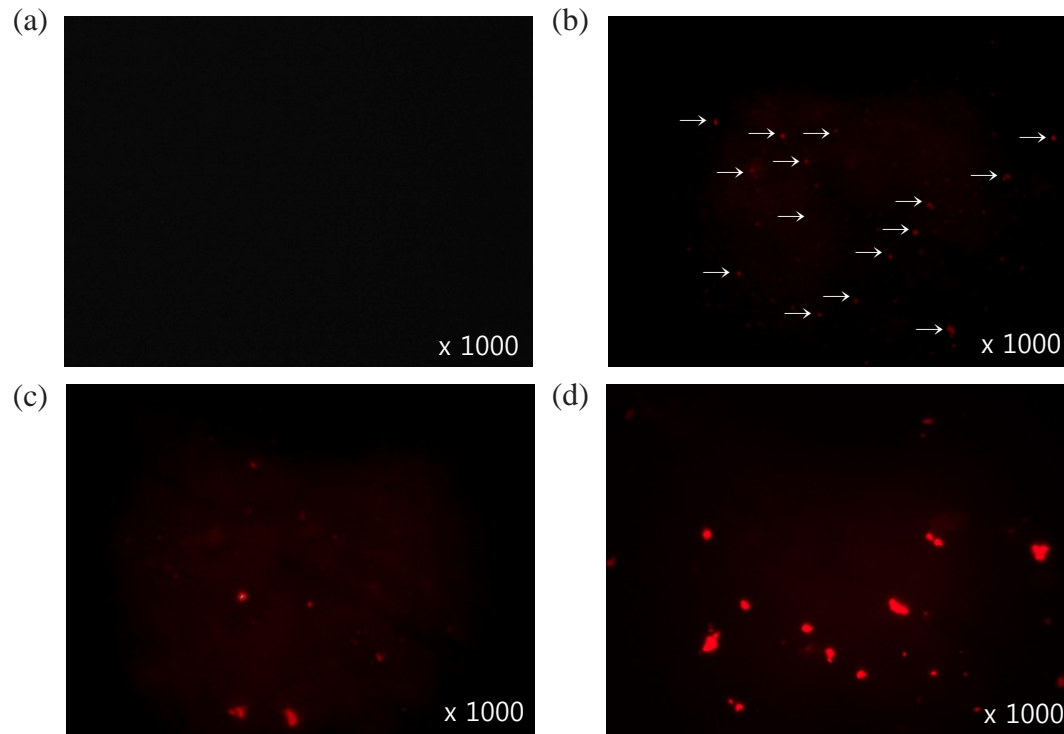


Fig. 10. Nile red fluorescence micrographs of 20 $\mu\text{g}/\text{mL}$ L- lactate dehydrogenase before and after freeze-thawing cycles for five times. The untreated LDH is represented in (a). The freezing rates were 0.2°C/min (white arrows indicate red particles) (b), 12.8°C/min (c), and 70.6°C/min (d).

3.4.3. Amyloid structure of the aggregates

Fluorescence analysis was used to estimate the structure of aggregates. In general, the intrinsic fluorescence of proteins stems from aromatic residues (D. Geddes, 2016); however, recent research has identified a new intrinsic protein fluorescence pattern in the visible range, even if excited in the UV region (Breydo & Uversky, 2014). This kind of fluorescence emission pattern is commonly observed in amyloid aggregates which have a high proportion of β -sheets (Chan, Kaminski Schierle, Kumita, Bertocini, Dobson, & Kaminski, 2013). The fluorescence was emitted in LDH treated with the different freezing rates, but was not observed in the untreated sample (Fig. 11). At the fastest freezing rate, the fluorescence intensity was significantly increased, indicating that a substantial amount of aggregates were formed. The aggregation degree of LDH increased as the freezing rate increased. This result demonstrated that aggregates rich in β -sheets were formed after freeze-thawing. However, it is unclear whether only amyloids were formed, or whether other aggregates also exist, because proteins can form aggregations with different structures such as amorphous aggregates, amyloid fibrils, and oligomers.

The amyloid formation could strengthen the assumption that the freezing process induced structural changes because proteins have to be partially or

completely unfolded in order for amyloid fibrillation to proceed (Breydo & Uversky, 2014; Murphy, 2007). The process of amyloid fibrillation of multimeric proteins could be triggered by changes in the quaternary structure of the proteins, and the dissociated monomers may have lower conformational stability than the tetramers, so that the monomers tend to be easily unfolded (Bulawa, et al., 2012). After the unfolded monomers are formed, they usually assemble into oligomers and undergo gradual conformational conversion to a β -sheet abundant conformation (Murphy, 2007). Oligomers having a high proportion of the β -sheet structure can also assemble into an amyloid structure (Breydo & Uversky, 2014). Since the formation of amyloid is accompanied by changes in the quaternary, tertiary, and secondary structure, LDH would have undergone structural changes in the freezing process.

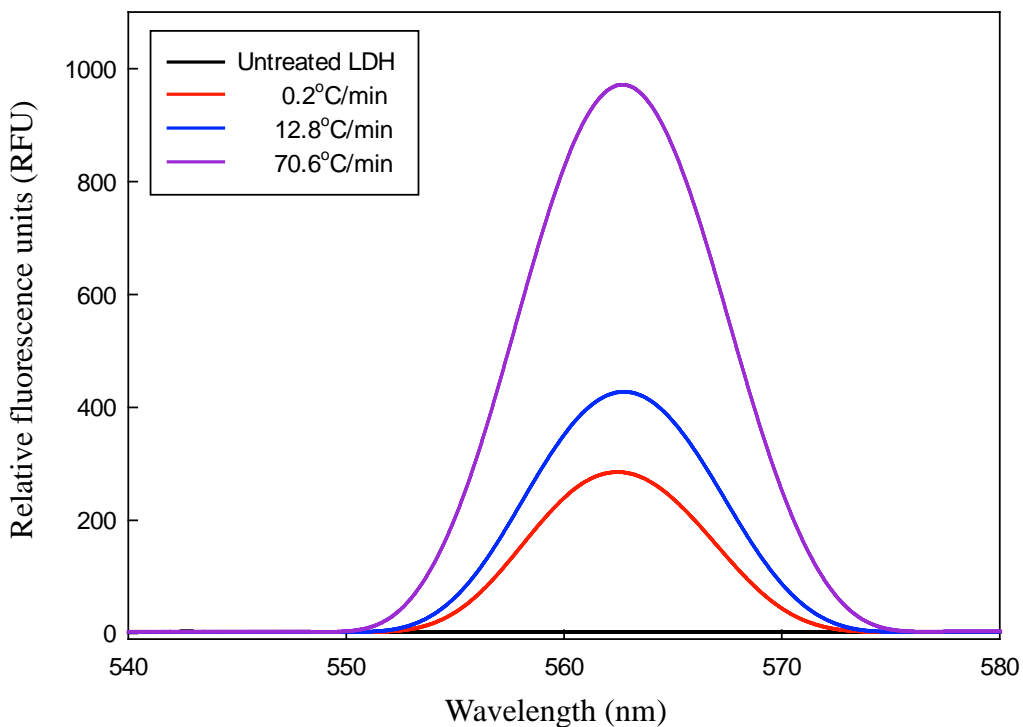


Fig. 11. Intrinsic fluorescence emission spectra of 20 $\mu\text{g/mL}$ L-lactate dehydrogenase before and after five freeze-thawing cycles at the visible range. The LDH solutions were frozen at 0.2, 12.8, and 70.6°C/min. The excitation wavelength was 280 nm.

4. Conclusion

This study showed that the enzyme activity decreased as the freezing rate increased above a specific freezing rate, and demonstrated that enzymes could be deactivated when they were placed at the ice/unfrozen solution interface. BN-PAGE and fluorescence spectroscopy showed that the changes in the quaternary and tertiary structure of the proteins increased as the freezing rate increased. The results from DLS analysis and fluorescence spectroscopy indicated that the size of aggregates tended to get larger as the freezing rate increased. Most of the aggregates were estimated to be of the amyloid form, since the fluorescence was emitted at the visible range.

In conclusion, this study identified optimal freezing rates with respect to enzyme activity when freezing enzymes. This study is valuable for elucidating the mechanism of enzyme deactivation during the freezing process.

5. Reference

- Anchordoquy, T. J., & Carpenter, J. F. (1996). Polymers protect lactate dehydrogenase during freeze-drying by inhibiting dissociation in the frozen state. *Archives of Biochemistry and Biophysics*, 332(2), 231-238.
- Anchordoquy, T. J., Izutsu, K. I., Randolph, T. W., & Carpenter, J. F. (2001). Maintenance of quaternary structure in the frozen state stabilizes lactate dehydrogenase during freeze-drying. *Archives of Biochemistry and Biophysics*, 390(1), 35-41.
- Bhatnagar, B. S., Bogner, R. H., & Pikal, M. J. (2007). Protein stability during freezing: Separation of stresses and mechanisms of protein stabilization. *Pharmaceutical Development and Technology*, 12(5), 505-523.
- Bhatnagar, B. S., Pikal, M. J., & Bogner, R. H. (2008). Study of the individual contributions of ice formation and freeze-concentration on isothermal stability of lactate dehydrogenase during freezing. *Journal of Pharmaceutical Sciences*, 97(2), 798-814.
- Brar, S. K., & Verma, M. (2011). Measurement of nanoparticles by light-scattering techniques. *TrAC, Trends in Analytical Chemistry*, 30(1), 4-17.

- Breydo, L., & Uversky, V. N. (2014). Molecular mechanisms of protein misfolding. In V. N. Uversky & Y. L. Lyubchenko (Eds.), *Bio-nanoimaging* (pp. 1-14). Boston: Academic Press.
- Bulawa, C. E., Connelly, S., Devit, M., Wang, L., Weigel, C., Fleming, J. A., Packman, J., Powers, E. T., Wiseman, R. L., Foss, T. R., Wilson, I. A., Kelly, J. W., & Labaudiniere, R. (2012). Tafamidis, a potent and selective transthyretin kinetic stabilizer that inhibits the amyloid cascade. *Proceedings of the National Academy of Sciences of the United States of America*, *109*(24), 9629-9634.
- Cao, E., Chen, Y., Cui, Z., & Foster, P. R. (2003). Effect of freezing and thawing rates on denaturation of proteins in aqueous solutions. *Biotechnology and Bioengineering*, *82*(6), 684-690.
- Chan, F. T., Kaminski Schierle, G. S., Kumita, J. R., Bertoncini, C. W., Dobson, C. M., & Kaminski, C. F. (2013). Protein amyloids develop an intrinsic fluorescence signature during aggregation. *Analyst*, *138*(7), 2156-2162.
- Chang, B. S., Kendrick, B. S., & Carpenter, J. F. (1996). Surface-induced denaturation of proteins during freezing and its inhibition by surfactants. *Journal of Pharmaceutical Sciences*, *85*(12), 1325-1330.
- D. Geddes, C. (Eds.). (2016). *Reviews in Fluorescence 2015* (1st ed. 2015, Vol. 5). Switzerland: Springer.

- Demeule, B., Gurny, R., & Arvinte, T. (2007). Detection and characterization of protein aggregates by fluorescence microscopy. *International Journal of Pharmaceutics*, 329(1-2), 37-45.
- Den, E. J., Garidel, P., Smulders, R., Koll, H., Smith, B., Bassarab, S., Seidl, A., Hainzl, O., & Jiskoot, W. (2011). Strategies for the assessment of protein aggregates in pharmaceutical biotech product development. *Pharmaceutical Research*, 28(4), 920-933.
- Dickinson, E. (1999). Adsorbed protein layers at fluid interfaces: Interactions, structure and surface rheology. *Colloids and Surfaces B: Biointerface*, 15(2), 161-176.
- Duy, C., & Fitter, J. (2006). How aggregation and conformational scrambling of unfolded states govern fluorescence emission spectra. *Biophysical Journal*, 90(10), 3704-3711.
- Franks, F. (1992). Freeze-drying: from empiricism to predictability. The significance of glass transitions. *Dev Biol Stand*, 74(9-18); discussion 19.
- Kasper, J. C., & Friess, W. (2011). The freezing step in lyophilization: Physico-chemical fundamentals, freezing methods and consequences on process performance and quality attributes of biopharmaceuticals. *European Journal of Pharmaceutics and Biopharmaceutics*, 78(2),

248-263.

Lorber, B., Fischer, F., Bailly, M., Roy, H., & Kern, D. (2012). Protein analysis by dynamic light scattering: methods and techniques for students. *Biochem Mol Biol Educ*, 40(6), 372-382.

Murphy, R. M. (2007). Kinetics of amyloid formation and membrane interaction with amyloidogenic proteins. *Biochimica et Biophysica Acta (BBA) - Biomembranes*, 1768(8), 1923-1934.

Permyakov, E., & Uversky, V. (2010). Fluorescence spectroscopy of intrinsically disordered proteins. In Hoboken, N. J., (Eds.), *Instrumental analysis of intrinsically disordered proteins: Assessing structure and conformation*. (pp. 323-344). New Jersey, Hoboken: Wiley.

Pikal-Cleland, K. A., Rodriguez-Hornedo, N., Amidon, G. L., & Carpenter, J. F. (2000). Protein denaturation during freezing and thawing in phosphate buffer systems: monomeric and tetrameric beta-galactosidase. *Archives of Biochemistry and Biophysics*, 384(2), 398-406.

Royer, C. A. (2006). Probing protein folding and conformational transitions with fluorescence. *Chemical Reviews*, 106(5), 1769-1784.

Schwegman, J. J., Carpenter, J. F., & Nail, S. L. (2009). Evidence of partial

- unfolding of proteins at the ice/freeze-concentrate interface by infrared microscopy. *Journal of Pharmaceutical Sciences*, 98(9), 3239-3246.
- Searles, J. A., Carpenter, J. F., & Randolph, T. W. (2001). The ice nucleation temperature determines the primary drying rate of lyophilization for samples frozen on a temperature-controlled shelf. *Journal of Pharmaceutical Sciences*, 90(7), 860-871.
- Wilson, P. W., Heneghan, A. F., & Haymet, A. D. J. (2003). Ice nucleation in nature: supercooling point (SCP) measurements and the role of heterogeneous nucleation. *Cryobiology*, 46(1), 88-98.
- Wittig, I., Braun, H.-P., & Schägger, H. (2006). Blue native PAGE. *Nature Protocols*, 1, 418.
- Zhang, A., Qi, W., Singh, S. K., & Fernandez, E. J. (2011). A new approach to explore the impact of freeze-thaw cycling on protein structure: hydrogen/deuterium exchange mass spectrometry (HX-MS). *Pharmaceutical Research*, 28(5), 1179-1193.

국문초록

본 연구는 모델 효소인 L-lactate dehydrogenase(LDH)에 대하여 동결 과정에서 동결 속도가 효소 활성에 미치는 영향을 확인하고, 최적의 동결 속도 조건을 제시하고자 하였다. 또한 동결 과정에서 효소적 활성이 손실되는 과정을 이해하기 위해 효소의 구조 변화를 분석하였다. 본 연구에서는 liquid-mediated freezing(LMF, 액체 매개 동결) 시스템을 구축하여 다양한 동결 속도에서 실험을 진행하였다. LMF는 초저온 냉동고에서 냉각된 isopropyl alcohol(IPA)속에서 샘플과 동시에 냉각하여 얼리는 기술이다. 샘플을 동결하기 직전의 IPA의 온도 변화를 통해 동결 속도를 조절하였다.

동결 속도 0.2 – 3.8°C/min 구간에서 LDH의 잔류 활성이 약 80%로 나타났고, 그 이상의 동결 속도 조건에서는 동결 속도가 빠를수록 유의적으로 활성이 감소하였다($p < 0.05$). 동결 속도 12.8, 70.6°C/min에서는 잔류 활성이 각각 64.1%, 44.8%로 나타났다. LDH의 4차 구조 변화는 blue native-PAGE 실험을 통해 분석하였고, 동

결 속도 70.6°C/min에서 tetramer와 dimer밴드의 세기가 감소 하였다. 이를 통해 동결 속도가 빠를 때 4차 구조의 변화가 크게 발생하는 것으로 보인다. 3차 구조 분석을 위한 fluorescence spectroscopy 결과에서는 동결 속도가 빠를수록 339 nm에서의 형광 강도가 유의적으로 감소하였다($p < 0.05$). 따라서 3차 구조의 변화도 동결 속도가 빠를 수록 증가하는 것으로 보인다.

또한 두 실험 결과 모두 동결 과정에서 단백질 응집 현상이 발생했을 가능성도 암시했다. LDH 용액의 크기 분포도는 dynamic light scattering(동적 광산란)을 통해 분석하였고, 동결 속도가 증가함에 따라 입자의 크기가 증가하였다. 형광 사진에서도 빠른 동결 속도에서 더 큰 단백질 응집체들이 생성되었다. 단백질 응집의 형태는 563 nm 부근에서 형광이 관찰되어 β -sheet 구조로 이루어진 amyloid 일 것으로 예상된다.

본 연구는 효소 동결 과정에서 동결 속도가 효소 활성화에 영향을 주는 요인임을 확인 하였고, 본 결과를 토대로 최적의 동결 속도 조건을 위한 가이드라인으로서 제시될 수 있다. 본 연구의 구조 분석 결과는 이후 연구에서 동결 과정에서 발생하는 효소 불활성화

메커니즘을 분석할 때 기초 연구로서 활용 될 수 있다.

Keywords: 동결, L-Lactate dehydrogenase, 동결 속도, 구조 변화,
단백질 응집

Student number: 2017-28564